Journal of Electrotechnology, Electrical Engineering and Management (2026)
Clausius Scientific Press, Canada

DOI: 10.23977/jeeem.2026.090116
ISSN 2560-6697 Vol. 9 Num. 1

A Study on Modeling and Control of Thermal Management Systems for Pure Electric Vehicles with Battery Temperature Control

Wenhao Li[a], Zhulin Zhang[b,*], Ruiyan Shi[c]

School of Automotive Engineering, Shandong Jiaotong University, Jinan, Shandong, China
[a]1184384977@qq.com, [b]qcxzhang@126.com, [c]2235160530@qq.com
[*]Corresponding author

Keywords: Pure electric vehicle; traction battery thermal management; integrated thermal management system; fuzzy control

Abstract: To address the cooling and preheating requirements of traction batteries in pure electric vehicles, this study proposes an integrated thermal management system coupling the refrigerant, battery, cabin heating, and motor/power-electronics cooling circuits. The system enables indirect natural cooling, chiller-assisted active cooling, and PTC-based low-temperature preheating of the battery. An AMESim/Simulink co-simulation model was developed, and a finite-state machine was used for operating-mode switching. A cooling-demand-based fuzzy controller was further designed, using cabin and battery cooling demands as inputs and a normalized compressor command as the output. By doing simulations with the WLTC (Worldwide Harmonized Light Vehicles Test Cycle), it was shown that under hot conditions the cabin temperature stayed around 22 ℃ and the battery temperature stayed near 32 ℃; under cold conditions, the cabin hit the target temperature within 500–600 seconds, while the battery temperature kept rising; compared with a common PID controller, the fuzzy control strategy made the start of cooling better and reduced the changes in cabin temperature and compressor speed, and these results suggest that the proposed system and strategy can help with battery temperature control and thermal management in pure electric cars.

1. Introduction

With the rapid development of pure electric vehicles, thermal management has become essential for vehicle safety, power performance, and driving range. Traction batteries are particularly temperature-sensitive. High temperatures accelerate degradation and increase thermal-safety risks, whereas low temperatures increase internal resistance and reduce available capacity and power capability[1-3].Effective battery cooling and low-temperature preheating are therefore critical for reliable operation under varying ambient conditions.

Conventional pure electric cars usually use separate circuits for cabin air conditioning, battery heat management, and electric-drive cooling; this separation limits heat sharing and coordinated control among subsystems; recent studies have therefore moved toward coupled and integrated heat management of the drive battery, cabin, and electric-drive system [4], such as improving liquid cooling plate design [5], developing models for battery heat with refrigerant [6], exploring motor waste heat recovery in whole systems [7,8], coordinating passenger comfort and battery temperature through direct refrigerant cooling and heating [9], and optimizing actuator control by dynamic programming [10].

Past studies have made a strong base for cooling batteries with liquid, managing heat with refrigerant, and handling heat for the whole vehicle; however, the systems that many people have designed depend on many valves, branch pipes, and working states, and this situation makes the system model and control execution become complicated.

To meet the thermal management requirements of traction batteries, this study proposes an integrated thermal management system for pure electric vehicles. The system provides chiller-based active battery cooling, PTC-based low-temperature preheating, and valve-based heat-flow regulation under different operating modes. A one-dimensional model is developed in AMESim and coupled with a finite-state machine and lower-level actuator controllers. Simulations are performed under high-temperature cooling, low-temperature heating, and dynamic driving conditions. Conventional proportional-integral-derivative control is further compared with a cooling-demand-based fuzzy control strategy to support system design and control optimization.

2. Architecture and Operating Modes of the Novel Thermal Management System

The proposed system integrates the refrigerant, cabin heating, battery thermal management, and motor/power-electronics cooling circuits, as shown in Figure 1.

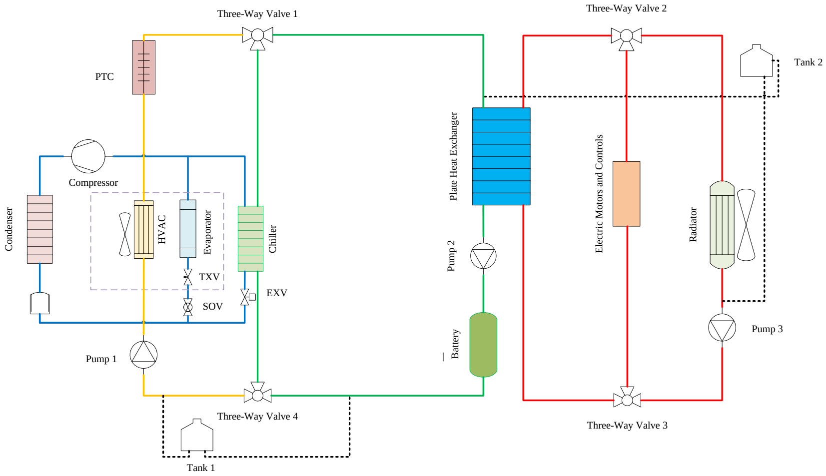

Figure 1. Architecture of the thermal management system

2.1 Overall System Architecture

The combined heat management system developed in this study (Figure 1) has four connected loops: refrigerant, cabin heating, battery temperature, and motor/power-electronics cooling loops [11]; they are linked through a chiller, a plate heat exchanger, and multi-port valves, and this lets heat be shared and modes switched. The refrigerant loop is for cabin cooling and active battery cooling, using the compressor, condenser, evaporator, chiller, and expansion parts; the cabin heating loop, with the PTC heater, Pump 1, and heater core, heats the cabin and preheats the battery under low temperatures.

The battery temperature loop provides indirect natural cooling, chiller-assisted active cooling, and PTC-based preheating; the motor/power-electronics cooling loop removes heat from the electric-drive system and rejects heat from the battery loop to the outside through the radiator; by making these loops work together, the design changes temperature-control modes with the ambient temperature and battery heat load, and this improves how it adapts to different conditions.

2.2 Design of the Battery Thermal Management Circuit

Traction-battery temperature strongly affects the power performance, safety, and energy efficiency of pure electric vehicles. The battery thermal management circuit is therefore treated as the core subsystem in the proposed architecture. It consists of the traction battery pack, Pump 2, plate heat exchanger, chiller, PTC heater, and three-way valves 1 and 4.

As shown in Figure 2, the circuit switches among three operating modes according to battery and ambient temperatures. In Mode (a), indirect natural cooling transfers heat from the battery circuit to the motor/power-electronics cooling circuit through the plate heat exchanger. In Mode (b), chiller-assisted active cooling uses the refrigerant circuit to cool the battery coolant. In Mode (c), PTC-based preheating raises the coolant temperature before it enters the battery pack.

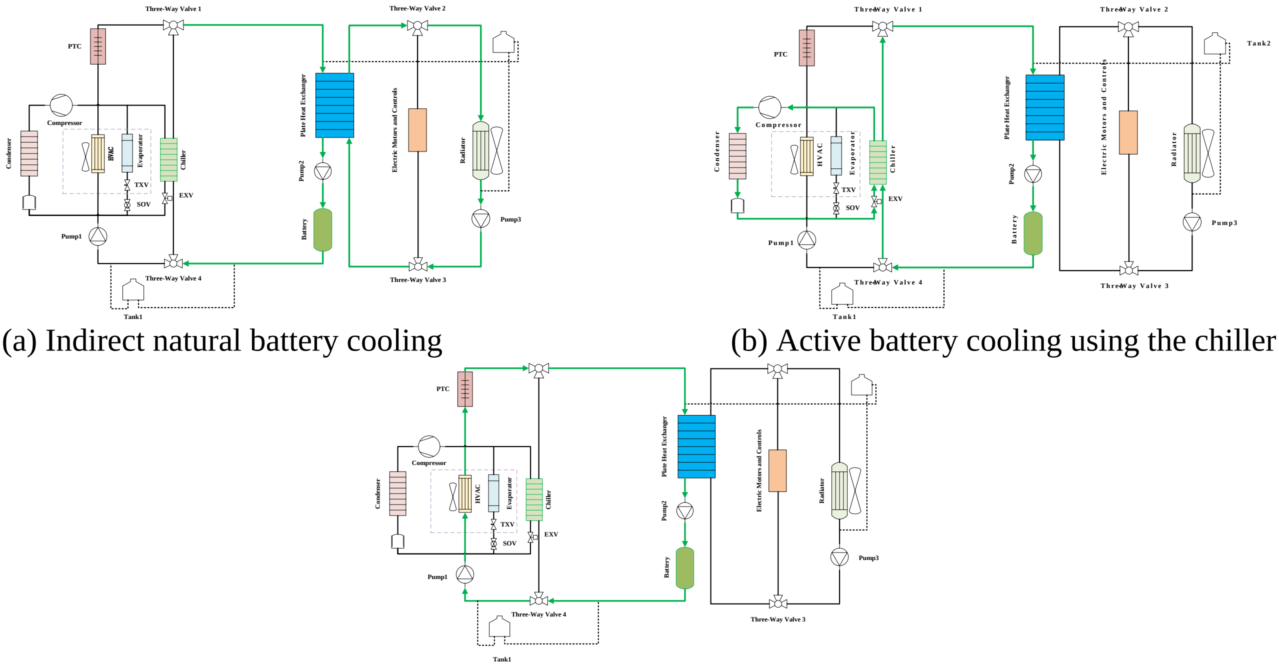

(a) Indirect natural battery cooling

(b) Active battery cooling using the chiller

(c) Low-temperature battery preheating using the PTC heater

Figure 2. Schematic diagram of the three operating modes of the battery thermal management circuit

2.2.1 Indirect Natural Battery Cooling Mode

The indirect natural cooling mode works when outside temperatures are moderate and the battery heat load is low; in this mode, Pump 2 pushes coolant through a plate heat exchanger, moving battery heat to the motor-electronics cooling circuit; then the radiator lets the heat out to the air; the refrigerant circuit is off, so the compressor uses less energy; when the battery temperature passes the active-cooling limit, the system changes to cooling with the chiller.

2.2.2 Active Battery Cooling Mode Using the Chiller

The active cooling mode turns on when outside temperatures are high or the battery heat load is high; in this mode, Pump 2 moves battery coolant through the chiller, and the low-temperature refrigerant absorbs its heat; the cooled coolant then goes back to the battery pack; compared with indirect natural cooling, this mode gives more cooling but uses more compressor energy; therefore, the compressor speed and expansion valve opening are controlled by the cooling needs of the battery and cabin together.

2.2.3 Low-Temperature Battery Preheating Mode Using the PTC Heater

The battery preheating mode is activated when the battery temperature falls below the specified threshold. In this mode, the valves connect the battery circuit to the PTC heating circuit, and the coolant pumps circulate heated coolant through the battery pack. The refrigerant circuit remains inactive during preheating. As the battery temperature approaches the target range, PTC heating power is reduced or switched off to limit energy consumption and prevent overheating.

2.3 Analysis of Typical Operating Modes

The system is divided into high-temperature cooling, moderate-temperature maintenance, and low-temperature heating regimes according to ambient temperature. Table 1 summarizes the corresponding thermal-management objectives and operating components.

Table 1. Typical operating modes and primary components of the thermal management system

Type	condition	Temperature-Controlled Object
cooling	Tamb>28℃	Cabin, battery, and motor/power electronics
maintenance	10℃≤Tamb≤28℃	Battery and motor/power electronics
heating	Tamb＜10℃	Cabin and battery

3. Control Strategy and Simulation Model Development

The physical thermal management system was modeled in AMESim, and the FSM and lower-level controllers were implemented in Simulink. A closed-loop AMESim/Simulink co-simulation was then used to evaluate performance under different operating conditions.

3.1 Development of the One-Dimensional AMESim Model

A one-dimensional AMESim model was developed for the proposed thermal management system, incorporating the heat-generation characteristics of major components and the coupled thermal circuits[12].The main vehicle parameters are listed in Table 2.

Table 2. Main vehicle parameters

Parameter	Unit	Value
Vehicle mass	kg	1520
Wheelbase	mm	2940
Tire		215/55R18
Frontal area	m2	2.46
Aerodynamic drag coefficient	-	0.28

3.1.1 Battery Heat-Generation Model

A lithium iron phosphate battery pack was used as the study object. During operation, the battery supplies electrical energy and generates heat through electrochemical reactions and ohmic losses.

Because battery voltage, current, and internal resistance can be measured experimentally, the Bernardi model was used to calculate the heat-generation rate.

$$q = I^2 R_{bat} + IT\frac{dU_{OCV}}{dT} \tag{1}$$

where q is the battery heat-generation rate; I is the discharge current; R_{bat} is the equivalent internal resistance; U_{OCV} is the open-circuit voltage; T is the battery temperature; and $\frac{dU_{OCV}}{dT}$ is the entropic coefficient.

3.1.2 Motor Heat-Generation Model

During operation, the motor converts electrical energy into mechanical energy. Copper losses, iron losses, and mechanical losses inevitably occur during this conversion process and are ultimately dissipated as heat. Therefore, the motor heat-generation rate can be calculated from the motor power and efficiency:

$$P_{mot} = P_m(1 - \eta_m) \tag{2}$$

where P_{mot} is the motor heat-generation rate, P_m is the motor power, and η_m is the motor efficiency..

3.1.3 Air-Conditioning System Model

The refrigerant circuit involves gas–liquid two-phase flow; therefore, simplified component models were developed to balance simulation accuracy and computational efficiency.

Compressor model: The refrigerant mass flow rate is calculated as:

$$q_m = \eta_v \rho_{suc} N D \tag{3}$$

where q_m is the refrigerant mass flow rate, η_v is the volumetric efficiency, ρ_{suc} is the suction density, N is the rotational speed, and D is the displacement.

Calculate the enthalpy change using isentropic efficiency:

$$\tau_{is} = \frac{q_m h_{inc} \eta_{mech}}{N} \tag{4}$$

where τ_{is} is the compressor torque, and η_{mech} is the compressor mechanical efficiency.

Heat Exchanger modeling: The evaporator and condenser are modeled as microchannel fin-and-tube heat exchangers.

The convective heat transfer between the refrigerant and the inner wall of the heat exchanger is expressed by Φ_{int}

$$\Phi_{int} = h_{ci} S(T_{ref} - T_{wall}) \tag{5}$$

where h_{ci} is the internal convective heat-transfer coefficient, S is the heat-transfer area, T_{ref} is the refrigerant temperature, and T_{wall} is the inner-wall temperature of the heat exchanger.

The heat-transfer correlation is selected according to the flow regime: the Gnielinski correlation is used for single-phase turbulent flow, the Shah correlation for condensation when $T_{ref} > T_{wall}$, and the Steiner correlation for flow boiling when $T_{wall} > T_{ref}$

External convective heat transfer occurs between the outer wall of the heat exchanger and the ambient humid air, as described by Φ_{ext}:

$$\Phi_{ext} = h_{ce} S(T_{air} - T_{wall}) \tag{6}$$

where h_{ce} and T_{air} denote the air-side heat-transfer coefficient and humid-air temperature, respectively.

The complete AMESim model is shown in Figure 3.

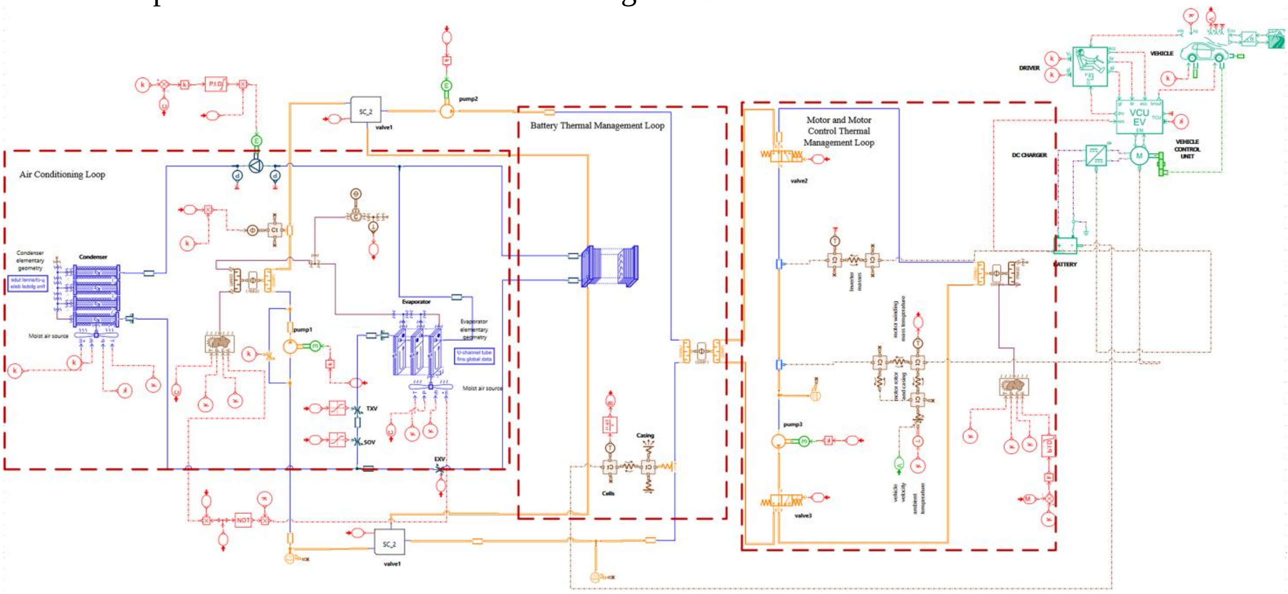

Figure 3. AMESim model of the vehicle thermal management system

3.2 Finite-State-Machine Control Strategy

Because the cabin, traction battery, and motor/power electronics have different thermal demands, a finite-state machine (FSM) is used for supervisory mode determination. As shown in Figure 4, the FSM first classifies the operating regime as high-temperature cooling, moderate-temperature maintenance, or low-temperature heating based on ambient temperature. It then identifies subsystem demands from the cabin, average battery, and motor/power-electronics temperatures.

The FSM outputs enable signals for cabin cooling or heating, indirect and active battery cooling, battery preheating, and motor/power-electronics cooling. Lower-level controllers regulate compressor speed, PTC heating power, and coolant-pump speed, whereas valve states are assigned according to the selected mode. This hierarchy separates discrete mode selection from continuous actuator control.

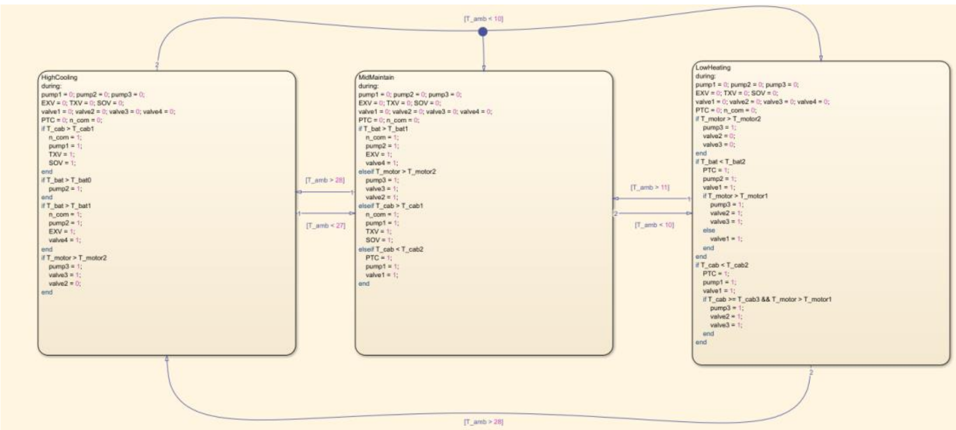

Figure 4. Operating-mode transitions of the finite-state machine

3.3 Lower-Level Actuator Control Strategy

Under the mode selected by the FSM, the lower-level controllers regulate the key actuators according to the thermal demand. Because compressor speed directly affects cabin cooling, battery-chiller capacity, and system energy consumption, conventional PID and cooling-demand-based fuzzy control are compared for compressor-speed regulation.

In conventional PID control, compressor speed is regulated using the cabin-temperature error $e(k)$ and its change $ec(k)$.

$$u_{PID}(k) = K_p e(k) + K_i \sum_{i=0}^{k} e(i) + K_d[e(k) - e(k-1)] \tag{7}$$

where $u_{\mathrm{PID}}(k)$ is the output of the PID controller, and K_p, K_i, and K_d are the proportional, integral, and derivative gains, respectively.

Because fixed-gain PID control has limited adaptability to varying thermal loads, a two-input fuzzy control strategy is introduced for compressor regulation.

The fuzzy controller uses cabin cooling demand AC and battery cooling demand BC as inputs and the normalized compressor control command DR as the output. AC BC and DR are normalized to $[0, 1]$.

The fuzzy subsets are {ZO,PS,PM,PB,PO} for AC and BC and {L,ML,M,MH,H,PO} for DR. The resulting fuzzy-control rules are listed in Table 3, with compressor output increasing with the combined cabin and battery cooling demand.

Table 3: Fuzzy Control Rules Table for the Compressor

Normalized Compressor Control Variables DR		Cabin Cooling Requirements AC				
		ZO	PS	PM	PB	PO
Battery Cooling Requirements BC	ZO	L	MH	H	H	PO
	PS	ML	H	H	PO	PO
	PM	M	H	PO	PO	PO
	PB	MH	H	PO	PO	PO
	PO	H	PO	PO	PO	PO

The inference surface of the compressor fuzzy controller derived from the fuzzy rules is shown in Figure 5. As the cabin cooling demand AC and battery cooling demand BC increase, the normalized compressor control command DR exhibits an overall upward trend. After speed mapping, the target compressor speed increases with the combined cooling demand of the system, thereby satisfying the coordinated cooling requirements of the passenger compartment and traction battery under high-temperature conditions.

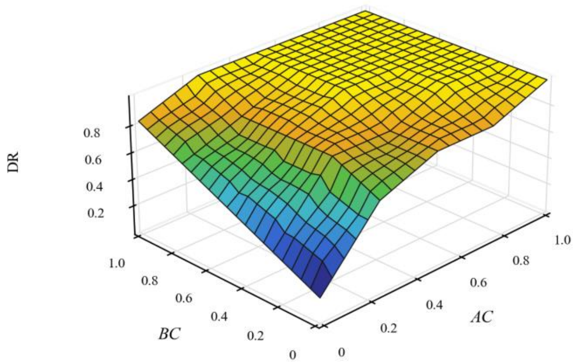

Figure 5. Inference surface of the compressor fuzzy controller

The target compressor speed can be expressed as follows:

$$\mathrm{n_{cmd}} = \mathrm{sat}[\mathrm{n_{min}} + \mathrm{DR}(\mathrm{n_{max}} - \mathrm{n_{min}})] \tag{8}$$

where n_{cmd} is the target compressor speed, $n_{\min}$ and $n_{\max}$are the allowable speed limits,and $\mathrm{sat}(.)$ denotes the saturation function.

The PID and fuzzy-control strategies are compared in Section 4.3 using cabin temperature, battery temperature, and compressor speed.

4. Simulation Results and Analysis under Typical Operating Conditions

4.1 High-Temperature Cooling Performance under the WLTC at Different Ambient Temperatures

To check how well the temperature is controlled under changing hot conditions, 1200-s WLTC simulations were run at ambient temperatures of 35, 40, and 45 ℃; Figure 6 shows the temperature responses.

At all three ambient temperatures, the cabin temperature dropped to about 21 ℃ within 100 s, then went up a little and stayed near 22 ℃; the battery temperature also kept dropping and became steady at about 32 ℃; higher ambient temperatures made the starting battery temperature and cooling load larger, and this made the time to reach a steady state longer; the WLTC load caused noticeable motor temperature changes, and the overall temperature level went up with ambient temperature; there was no temperature rise that kept going without control, showing that the motor cooling circuit kept heat from building up under dynamic loads; however, high ambient temperature still had a big effect on the motor thermal state.

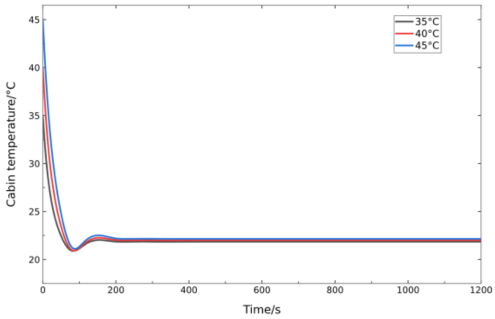

(a) Passenger-compartment temperature response

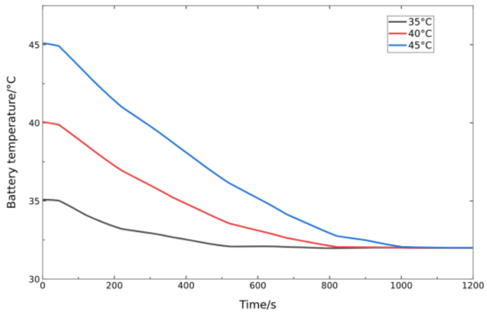

(b) Battery temperature response

Figure 6. Temperature responses during cooling at different ambient temperatures

4.2 Low-Temperature Heating Performance under the WLTC at Different Ambient Temperatures

To see how the heating performed under changing low-temperature conditions, 1200-s WLTC simulations were run at ambient temperatures of -10, -5, and 0 ℃; the temperature responses of the cabin and battery are given in Figure7.

Under all three conditions, the cabin temperature kept rising and hit about 22 ℃ within 500-600 s; higher ambient temperatures made the heating time shorter, with the 0 ℃ case reaching the target first; after that, it changed a little around the target and stayed stable.

The battery temperature went up steadily during the simulation, with faster heating at warmer ambient temperatures; at the end, the battery temperatures reached about 8, 10, and 12 ℃ at -10, -5, and 0 ℃; in the -10 ℃ case, the battery did not get to 10 ℃, showing that severe cold increased the preheating load and delayed getting into the right working range.

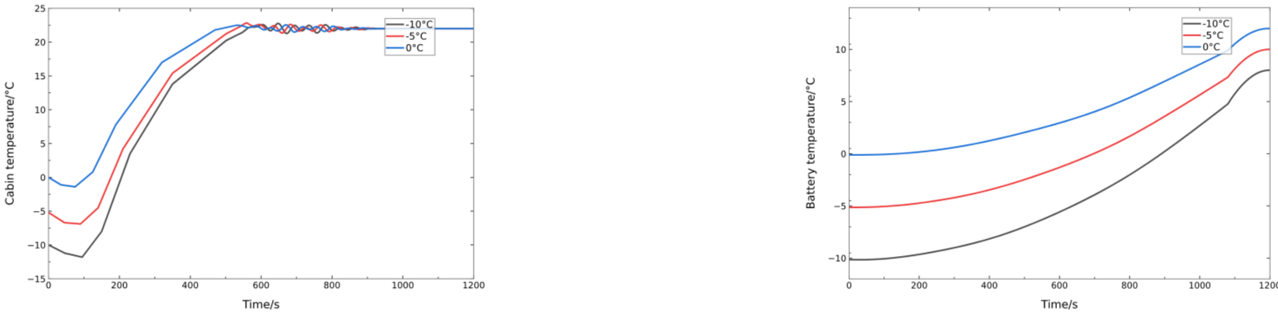

(a) Passenger-compartment temperature response (b) Battery temperature response

Figure 7. Temperature responses during heating at different ambient temperatures

4.3 Comparison between PID and Fuzzy Control

To evaluate compressor-speed regulation, conventional PID and cooling-demand-based fuzzy control were compared under the same high-temperature WLTC cooling condition. The system parameters, initial states, and external loads were identical, and only the compressor-speed control method differed. The passenger-compartment temperature, battery temperature, and compressor-speed responses are shown in Figure 8.

Both strategies reduced the passenger-compartment temperature to approximately 22 ℃. Fuzzy control achieved a faster initial cooling response, a smaller temperature undershoot, and a smoother recovery than PID control. After the target temperature was reached, fuzzy control also reduced residual temperature fluctuations and stabilized the passenger compartment more rapidly.

The battery had a larger ability to store heat, so its temperature changed more smoothly; under fuzzy control, the battery temperature dropped faster at first, because the compressor gave more output when cooling demand was high; both control ways later made the battery temperature stay near 32 ℃; but fuzzy control caused a clear drop below the target around 800-900 s, and this means the battery cooling demand settings still need to be made better; the compressor ran at a high speed in the starting period and then slowed down when the cooling load got smaller; the fuzzy controller changed its DR control number following the cooling needs of the cabin and battery; a bigger DR kept the compressor speed higher when demand was high, while a smaller DR cut the speed when demand went down; compared with PID control, which had strong speed swings after 600 s, fuzzy control gave a compressor speed that was more smooth and steady; overall, fuzzy control made the cooling start better and reduced the ups and downs in cabin temperature and compressor speed during steady state; these results show that it can adapt better and stay stable under hot WLTC driving.

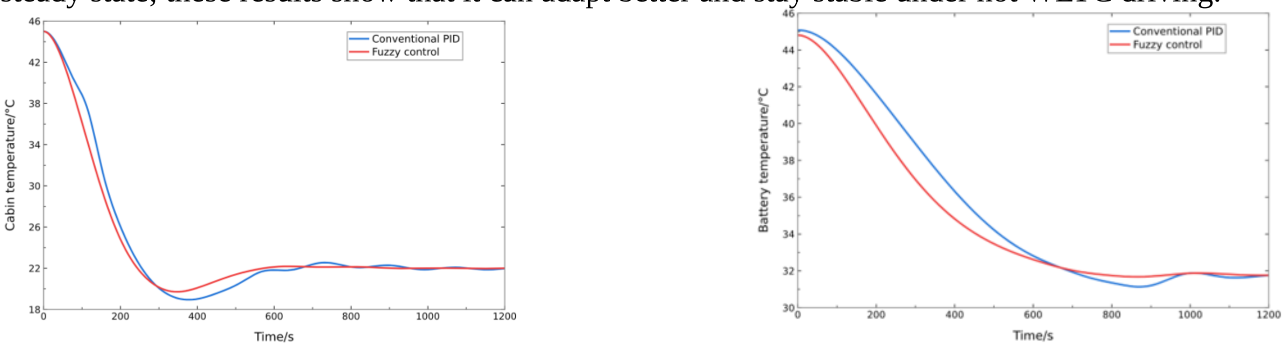

(a) Passenger-compartment temperature response (b) Battery temperature response

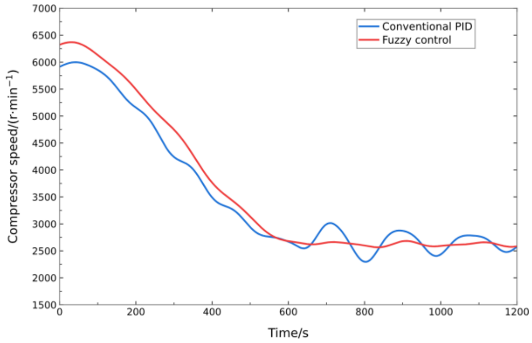

(c) Compressor-speed response

Figure 8. Comparison of PID and fuzzy control performance

5. Conclusions

The study developed an integrated thermal management system for pure electric vehicles to address traction-battery cooling and preheating requirements. An AMESim/Simulink co-simulation model was established and combined with a hierarchical control strategy. WLTC simulations at different ambient temperatures and a comparison between PID and fuzzy control led to the following conclusions.

(1) The proposed system achieved indirect natural cooling, chiller-assisted active cooling, and PTC-based low-temperature preheating for the traction battery. It also met cabin cooling/heating demands and motor/power-electronics heat-dissipation requirements under typical high-, moderate-, and low-temperature conditions.

(2) Under high-temperature WLTC cooling conditions, the passenger-compartment temperature stabilized at approximately 22 ℃, and the battery temperature stabilized near 32 ℃. Although motor temperature increased with ambient temperature, no sustained uncontrolled rise occurred.

(3) Under low-temperature WLTC heating, the cabin temperature reached about 22 ℃ in 500-600 s; the battery temperature kept rising, but the heating speed dropped at lower ambient temperatures; at -10 ℃, the battery did not get to 10 ℃, showing that PTC heating ability should be improved for very cold conditions.

(4) Compared with PID control, the fuzzy strategy based on cooling demands made a compressor command from cabin and battery needs; this improved the initial cooling response and reduced cabin temperature and compressor-speed fluctuations; however, a small battery undershoot remained, meaning the fuzzy rules and membership-function parameters need further optimization; Overall, the integrated thermal management system met vehicle temperature-control needs under typical conditions; the cooling-demand-based fuzzy control strategy showed better dynamic response and stability than PID, supporting further design and control optimization.

In general, under typical working conditions, the vehicle’s temperature-control needs were met by the combined thermal management system.The cooling-demand-based fuzzy control strategy showed better dynamic response and operational stability than PID control, supporting further structural design and control optimization.

References

[1] KIM J, OH J, LEE H. Review on battery thermal management system for electric vehicles[J]. Applied Thermal Engineering, 2019, 149: 192-212.

[2] JAGUEMONT J, BOULON L, DUBÉ Y. A comprehensive review of lithium-ion batteries used in hybrid and electric vehicles at cold temperatures[J]. Applied Energy, 2016, 164: 99-114.

[3] XIA G, CAO L, BI G. A review on battery thermal management in electric vehicle application[J]. Journal of Power

Sources, 2017, 367: 90-105.
[4] LEI S, XIN S, LIU S. Separate and integrated thermal management solutions for electric vehicles: A review[J]. Journal of Power Sources, 2022, 550: 232133.
[5] JARRETT A, KIM I Y. Design optimization of electric vehicle battery cooling plates for thermal performance[J]. Journal of Power Sources, 2011, 196(23): 10359-10368.
[6] SHEN M, GAO Q. System simulation on refrigerant-based battery thermal management technology for electric vehicles[J]. Energy Conversion and Management, 2020, 203: 112176.
[7] TIAN Z, GU B. Analyses of an integrated thermal management system for electric vehicles[J]. International Journal of Energy Research, 2019, 43(11): 5788-5802.
[8] TIAN Z, GU B, GAO W, et al. Performance evaluation of an electric vehicle thermal management system with waste heat recovery[J]. Applied Thermal Engineering, 2020, 169: 114976.
[9] GUO J, JIANG F. A novel electric vehicle thermal management system based on cooling and heating of batteries by refrigerant[J]. Energy Conversion and Management, 2021, 237: 114145.
[10] LIAN Y B, LING H P, ZHU J P, et al. Thermal management optimization strategy of electric vehicle based on dynamic programming[J]. Control Engineering Practice, 2023, 137: 105562.
[11] HE L, JING H, ZHANG Y, et al. Performance research of integrated thermal management system for battery electric vehicles with motor waste heat recovery[J]. Journal of Energy Storage, 2024, 84: 110893.
[12] HONG J, SONG J, HAN U, et al. Performance investigation of electric vehicle thermal management system with thermal energy storage and waste heat recovery systems[J]. eTransportation, 2024, 19: 100317.